**Technical Paper**

ISSN 1997-1400 Int. J. Pavement Res. Technol. 7(4):247-255


# Utilizing Asphaltic Concrete Overlay to Mitigate the Detrimental Effects of Alkali Carbonate Reactions in Portland Cement Concrete Pavement

Kevin Gaspard[1+], Zhongjie Zhang[1], Tyson Rupnow[1], and Patrick Icenogle[1]

**Abstract:** In 1990, the Louisiana Department of Transportation and Development (LADOTD) constructed approximately 9.96 km of portland cement concrete (PCC) pavement on Interstate 20. In 1994, the PCC began to show signs of distress in the form of surface cracks, joint spalling, pop outs, and efflorescence.

Alkali carbonate reactions (ACR) in the PCC were discovered upon analyzing cores taken from the PCC in 1996. In 1997 and 1998, LADOTD placed a 102-mm AC overlay on the PCC pavement on the east- and west- bound lanes, respectively. Sawing and sealing the AC over the PCC joints was performed to mitigate reflective cracking. The AC overlay added structure to the pavement section reducing stress on the PCC, created a barrier preventing surface moisture from entering into the PCC, and created a thermally insulated pavement reducing the temperature within the PCC.

Pavement surface distress data was obtained by data mining the LADOTD Pavement Management system data base and structural testing the composite pavement was conducted with the Falling Weight Deflectometer. Cores were obtained from the PCC and tested in accordance with a modified ASTM C1567-13 in October 2012.

Approximately 15 years after the placement of the AC overlay, only minimal transverse cracking, longitudinal cracking, and patching were discovered and the roadway had a smooth ride. Results from the structural testing indicated that the PCC pavement was distressed with the overall structural number of the pavement being approximately 5.5. When tested in accordance with a modified ASTM C1567-13, significant volumetric strains up to 0.8 percent were measured on the PCC cores. Volumetric strains of that magnitude will cause detrimental effects on the PCC, eventually leading to its destruction.

**DOI**: 10.6135/ijprt.org.tw/2014.7(4).247

***Key words****: Alkali Aggregate reaction; Alkali Carbonate reaction; Composite Pavement; PCC performance; PCC rehabilitation.*

## Introduction /Literature Review

In 1990, the Louisiana Department of Transportation and Development (LADOTD) constructed approximately 9.96 km of portland cement concrete (PCC) pavement on Interstate 20 (I-20) in Lincoln Parish. The pavement typical section consisted of 330-mm PCC, 51-mm asphaltic concrete (AC) base course, and 216-mm soil cement subbase. It has a current ADT of approximately 34,700 with 20 percent trucks and a skewed joint spacing of 6.1-m. In 1994, the PCC began to show signs of distress in the form of surface cracks, joint spalling, popouts, and efflorescence similar to the photos presented in Fig. 1.

Cores were initially taken in 1996 and upon analysis by the United States Army Corps of Engineers, it was determined that the culprit was Alkali Carbonate Reaction (ACR). Coring was conducted again in 2012 and will be discussed later in this report.

Alkali-Carbonate Reactive aggregates in PCC were first catalogued in 1957 [1-2]. ACR along with Alkali-Silica Reaction (ASR), are routinely referred to as Alkali-Aggregate Reaction (AAR) [1-12]. ACR is less common than ASR with only a few isolated locations worldwide documenting its existence [4]. Though different thermodynamic-chemical-mechanical processes drive ACR and ASR, similar mitigation strategies have been used for both [1-32].

Alkali hydroxides (2KOH or 2NaOH) in cement interact with certain matrices of fine calcite and clay minerals in argillaceous dolomitic limestones to produce ACR, which leads to PCC distresses such as cracking, loss of strength, spalling, popouts, and efflorescence usually within five years of construction [1-12]. Eq. (1) represents the dedolomitization process, though the specific geochemical processes are not fully understood at this time. Note that the soluble carbonates are available to participate in further dedolomitization reactions.

$$CaMg(CO_3)_2 + 2ROH \rightarrow CaCO_3 + Mg(OH)_2 + R_2CO_3 \qquad (1)$$

dolomite + alkali hydroxide → calcite + brucite + soluble carbonate with R representing either K or Na.

**Fig. 1.** PCC Distresses.

[1] Louisiana Transportation Research Center, Louisiana State University, 4101 Gourrier Ave., Baton Rouge, LA 70808, USA.

[+] Corresponding Author: E-mail kevin.gaspard@la.gov

Note: Submitted February 19, 2014; Revised April 1, 2014; Accepted April 6, 2014.

Mechanisms in addition to reactive aggregate that drive the AAR (ACR or ASR) processes are (1) sufficient moisture to keep the relative humidity within the PCC above 80 percent, (2) high alkali contents (> 2.4 kg per cubic meter) in the PCC, and (3) elevated temperatures [1-12]. Any mechanism or treatment that shields the PCC from surface or subsurface water intrusion, inhibits high temperatures, and prevents alkali intrusions will retard the AAR process.

The expansion stresses ($\sigma$) that occur within the PCC are equal to the tensile stress ($\sigma_\mu$) capacity of the internal PCC matrix minus the swelling pressure ($p_g$) caused by the reactive aggregate as presented in Eq. (2) and Fig. 2 [1-12]. When the expansion stresses (σ) exceed the tensile stress ($\sigma_t$) of the PCC matrix ($\sigma > \sigma_t$), microcracks propagate radially from the aggregate in a random fashion. The combination of the swelling and microcracks leads to the deterioration and eventual destruction of the PCC matrix.

$$\sigma = \sigma_\mu - p_g \tag{2}$$

with,
$\sigma$ = stress caused by expansion
$\sigma_\mu$ = tensile stress resisting swelling pressure
$p_g$ = swelling pressure.

Mitigating AAR once PCC pavement has been constructed is problematic [7, 13-16]. There are several chemical treatment approaches to deal with AAR issues. Lithium has been shown to retard the AAR process in the laboratory [7, 13-14]. On field projects, it has limited usefulness since it was shown to only penetrate 3 mm into the PCC after three treatments [7, 13-14]. Siloxanes and silanes have been used in an attempt to retard the ingress of surface water into the PCC pavement. However, they are only able to penetrate approximately 6 mm into the PCC surface and provide no shielding from subsurface water entering into the PCC pavement [7, 15-16]. Due to their inability to penetrate significantly into the PCC, lithium, siloxanes, and silanes have been ineffective in mitigating AAR in existing PCC pavements [4, 7, 13-16].

Rubblizing the PCC (RPCC) and overlaying with asphaltic concrete (AC) has been proven to be an effective method of mitigating the adverse effects of AAR pavements [17-24]. Colorado reported that after seven years of service, there were no surface distresses such as transverse cracks, settlement, or permanent deformation [20].

Another method of dealing with the AAR issue is to overlay the PCC with AC to create a composite pavement, the topic of this paper. In 1997 and 1998, LADOTD placed a 102 mm AC overlay on the PCC pavement on the East and West bound lanes, respectively. Sawing and sealing the AC over the PCC joints was performed to mitigate reflective cracking [27].

The AC overlay serves many purposes. It acts as a thermal insulator to the PCC pavement as well as retards surface water from entering the PCC [25-28]. Shielding the PCC from high temperatures as well as minimizing surface water intrusion reduces the ACR process and its detrimental effects. Additionally, the AC overlay adds structural strength to the pavement section which in turn, reduces stress on the PCC pavement.

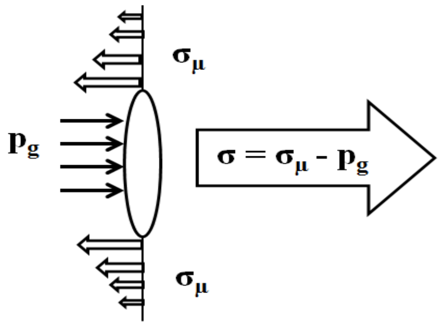


**Fig. 2.** Expansion Stress Model for PCC Matrix.

**Table 1.** PMS Test Data.

| East Bound Lanes | | West Bound Lanes | |
|---|---|---|---|
| Test Date (1) | Age (2) | Test Date (1) | Age (2) |
| 6/23/1997(3) | 0.0 | 4/29/1998(3) | 0.0 |
| 3/30/1998 | 0.8 | 6/30/1998 | 0.2 |
| 3/30/2000 | 2.8 | 3/30/2000 | 1.9 |
| 1/20/2003 | 5.6 | 1/20/2003 | 4.7 |
| 9/14/2008 | 11.2 | 3/25/2005 | 6.9 |
| 10/7/2010 | 13.3 | 5/25/2007 | 9.1 |
| 10/11/2012 | 15.3 | 9/25/2008 | 10.4 |
| | | 10/7/2010 | 12.4 |
| | | 10/11/2012 | 14.5 |

Legend: (1) Date of Test, (2)Age of AC Overlay (years), (3) Initial Construction of AC Overlay in Years.

Another source of moisture to aide in the ACR process comes from the subgrade. This moisture path can be mitigated by inserting underdrains adjacent to the pavement [31-32]. However, this was not attempted on I-20.

## Research Methodology/Design of Experiment

### Functional Distresses

The authors began by data mining the LADOTD pavement management system (PMS) data base to obtain the pavement surface distress and ride quality (International Roughness Index (IRI)) history of this section of I-20 [28]. Data collection took place in the outside lanes for both the east and west bound lanes and no treatments other than the AC overlay took place on those lanes for the dates presented in Table 1. For composite pavements, PMS catalogues and stores transverse cracks, longitudinal cracks, patching, and International roughness index (IRI) data [27-32]. Because there were only minimal amounts of transverse cracks, longitudinal cracks, and patching between the initial overlay and 2012, only IRI data were statistically analyzed. Table 1 presents the dates that data was available for the statistical analysis.

For the IRI data, a regression analysis was conducted to develop a model to establish the relationship between the response variable ($Y_i$) and the explanatory variable ($X_i$) at the alpha = 0.05 percent level [33]. Confidence and prediction intervals were computed and plotted with the least squares regression line for each analysis. The confidence interval (CI) represents the range of the means from multiple tests that can be expected from field sampling while the

**Fig. 3.** PCC Cores.

prediction interval (PI) represents the expected range of a single value obtained from field sampling [33].

The regression model used in this analysis is presented in Eq. (3).

$$Y_i = \beta_0 + \beta_1 * X_i \tag{3}$$

where,
$Y_i$ = functional distress (IRI cm/km)
$\beta_0$ = intercept
$\beta_1$ = regression coefficient for $X_i$
$X_i$ = age (years)

## Structural Distresses

The Falling Weight Deflectometer (FWD) was used to access the strength of the pavement structure. From its tests, the pavement layer moduli and the in-place structure number ($SN_{eff)}$ were determined [31-36]. The pavement layers for this project consisted of 102-mm AC, 330- mm jointed PCC, 51-mm AC base course, 216-mm soil cement subbase, and subgrade. Though this constitutes a 5 layer system, the backcalculation process would only allow for four layers to be assessed [35]. Moduli were determined for the 102-mm AC layer, 330-mm PCC layer, 51- mm AC base course, and subgrade, which in this case was a composite of the 216-mm soil cement subbase and subgrade.

FWD tests were conducted on two occasions at similar locations on May 2007 and October 2012. An Analysis of Variance (ANOVA) statistical test using Tukey's method was performed at alpha = 0.05 to determine if statistical differences existed between test dates for the pavement layer moduli and $SN_{eff}$ parameters [33].

## PCC Core Sampling

The Louisiana Transportation Research Center (LTRC) sampled the I-20 pavement section in 17 locations by obtaining eight 150-mm diameter and nine 100-mm diameter cores in October 2012 as presented in Fig. 3 and Table 2. In areas where the cores remained intact, cracks ranging from mild to severe were observed originating from aggregates and in some locations dark rims around the aggregate were observed as presented in Table 2. This is indicative of ACR [1-12]. Six cores were laboratory tested in accordance with ASTM C1567-13 with the following exceptions, concrete cores were tested instead of mortar bars, length and diameter change were recorded, and testing was conducted for a period of 56 days [37]. Based upon the condition of the cores, three 150-mm diameter cores were tested in water and two 150-mm diameter and one 100-mm diameter cores were tested in a sodium hydroxide (NaOH) solution as presented in Table 2 [37]. The resulting length, diameter and volumetric strains, Eqs. (4), (5), and (6), were calculated, plotted, and statistically analyzed using Tukey's method at alpha = 0.05 [33].

**Table 2.** PCC Core Condition**.**

| Core No. / Diameter (mm) | PCC Core Condition after Retrieval from Hole | Cracking in PCC | Lab Tested |
|---|---|---|---|
| 1 / 150 | Retrieved about 178 mm of Core from Hole. | Light Cracks in Core. | n.a. |
| 2 / 100 | Only the AC Layer was Extracted. | Unknown. | n.a. |
| 3 / 100 | Core Extracted in Two Pieces, 102 mm and 229 mm in Length. | Cracks Originating from Large Aggregates. | n.a. |
| 4 / 100 | Material Destroyed in Process Due to Poor Core Barrel. | Unknown. | n.a. |
| 5 / 100 | Core Extracted in Two Pieces with Top 75 mm Portion Crumbling. | Some Separation between Aggregates and Paste in Top 75mm Portion. | NaOH |
| 6 / 100 | Core Retrieved but Crumbled into Large Pieces Ranging from 25 to 50 mm in Length | Some Separation between Aggregates and Paste Throughout the Core. | n.a. |
| 7 / 100 | Core Extracted from Hole. | Cracking Throughout Core. | n.a. |
| 8 / 100 | Retrieved about 152 mm of Core from Hole. | Cracking Throughout Core. | n.a. |
| 9 / 100 | Retrieved about 203 mm of Core from Hole | Cracking Throughout Core. | n.a. |
| 10 / 100 | Core Broke into Many Pieces. | Unknown. | n.a. |
| 11 / 150 | Core Extracted Intact. | Cracks Originating from Large Aggregates. | $H_2O$ |
| 12 / 150 | Core Extracted in Two Pieces, 76 mm and 254 mm in Length. | Cracks Originating from Large Aggregates. | $H_2O$ |
| 13 / 150 | Core Extracted in Two Pieces, 102 mm and 229 mm in Length. | Cracks Originating from Large Aggregates. | $H_2O$ |
| 14 / 150 | Core Extracted Intact. | Light Cracking at Bottom Portion of Core. | NaOH |
| 15 / 150 | Retrieved about 216 mm of Core. | Light Cracking in Core. | NaOH |
| 16 / 150 | Retrieved about 216 mm of Core. | Light Cracking and Dark Rim Around Aggregates. | n.a. |
| 17 / 150 | Retrieved about 50 mm of Core. | Unknown. | n.a. |

Legend: $H_2O$ – water, NaOH – sodium hydroxide

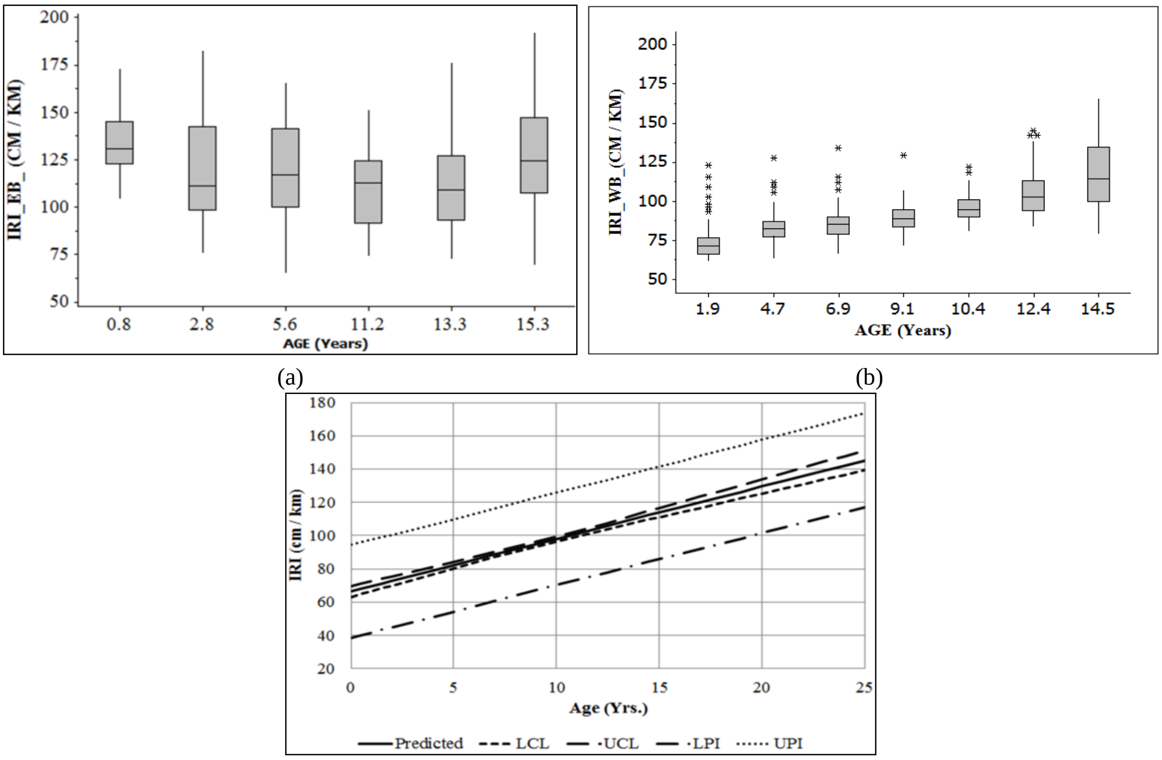


(c)

**Fig. 4.** Regression Analysis results: (a) Boxplots of EB IRI Data Set, (b) Boxplots of WB IRI Data Set, (c) Regression Line for WB IRI Data, (UCL – Upper Confidence Limit, LCL – Lower Confidence Limit, UPI – Upper Prediction Interval, and LPI – Lower Prediction Interval).

$\varepsilon_l$ = *change in length of specimen / original length of specimen* * 100   (4)

with $\varepsilon_l$ = strain of length in percent

$\varepsilon_d$ = *change in diameter of specimen / original diameter of specimen* * 100   (5)

with $\varepsilon_d$ = strain of diameter in percent

$\varepsilon_v$ = *change in volume of specimen / original volume of specimen* * 100   (6)

with $\varepsilon_v$ = strain of volume in percent

## Analysis of Results

### Functional Distress

Regression modeling on the IRI data for east bound and west bound lanes indicated that a statistically significant relationship existed for the west bound lane but not the east bound lane as presented in Fig. 4a to 4c. The regression equation for the west bound lane is presented in Eq. (7).

*IRI* (cm/km) = 66.58 + 3.1494**Age* (yrs.)   (7)

For the east bound lanes, the regression model was not significant, which means from a statistical standpoint, the IRI (1997- 2012) did not significantly change during that 15.3 year period. Because of that, an equation to predict the future IRI values was not developed. The average IRI for all years in the east bound lane was approximately 95 cm/km.

**Table 3.** Ride Quality.

| Ride Quality | IRI (cm/km) |
|---|---|
| Smooth | ≤ 126 |
| Moderate | 127 to 204 |
| Rough | ≥ 205 |

According to FHWA, the IRI limits presented in Table 3 can be used to define ride quality [30]. Using that as a guide, both the east and west bound lanes currently have a smooth ride. According to the regression equation for the west bound lanes, the ride will remain in the smooth category until approximately 19 years of age.

### Structural Distresses

#### *East Bound Roadway*

Cumulative frequency distribution percent histograms for the parameters of AC, PCC, AC base course, subgrade, and $SN_{eff}$ were constructed for the test dates of May 2007 and October 2012 as presented in Fig. 5a to 5e. An ANOVA for each parameter comparing test dates was conducted and is presented in Table 4. With the exception of the AC base course, statistical similarities were discovered for the parameters at the two test dates. This infers that the pavement structure did not deteriorate in the five year period between May 2007 and October 2012. Unfortunately, structural data was not available from earlier years in the pavements service life so the authors could not determine if it had loss strength from the time of its construction.

Generally, concrete pavements in good condition have modulus

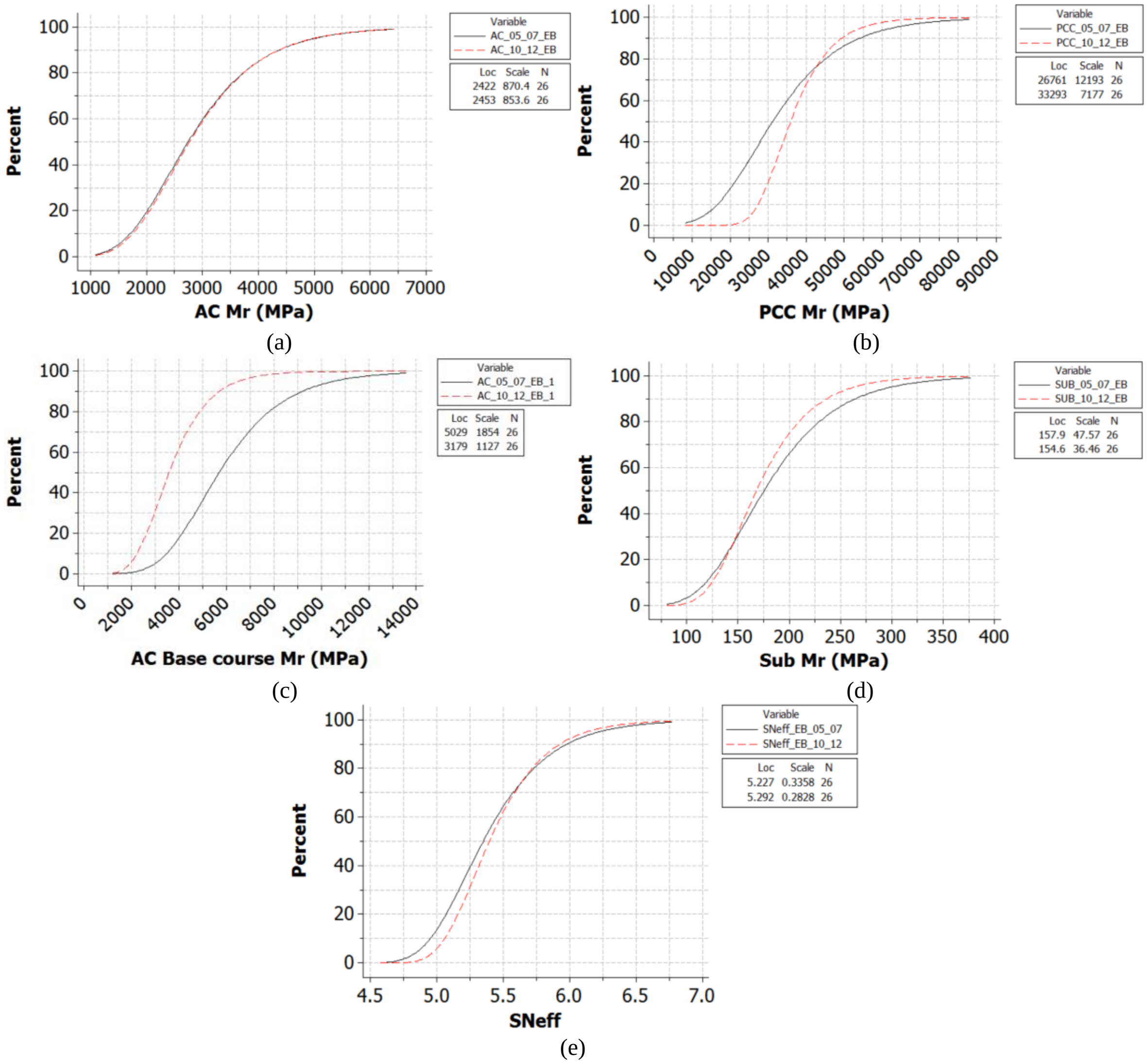


**Fig. 5.** East Bound Histograms: (a) $M_r$ of AC Pavement, (b) $M_r$ of PCC Pavement, (c) $M_r$ of AC Base Course, (d) $M_r$ of Subgrade, (e) $SN_{eff}$ of Pavement Layers.

values in excess of 27,579 MPa [27-28, 31-32]. On the east bound side in May 2007, approximately 39 percent of the slabs tested had modulus values lower than 27,579-MPa and in October 2012, approximately 10 percent had modulus values less than 27,579-MPa as presented in Fig. 5b. Based upon these modulus results, it can be concluded that the PCC is distressed.

### *West Bound Roadway*

Cumulative frequency distribution percent histograms for the parameters of AC, PCC, AC base course, subgrade, and $SN_{eff}$ were constructed for the test dates of May 2007 and October 2012 as presented in Fig. 6a to 6e. An ANOVA for each parameter comparing test dates was conducted and is presented in Table 4. Statistical similarities were discovered for all parameters at the two test dates. This implies that the pavement structure did not deteriorate in the five-year period between May 2007 and October 2012. Unfortunately, structural data was not available from earlier times in the pavements service life so the authors could not determine if it had loss strength from the time of its construction.

On the west bound side in May 2007, approximately 9 percent of the slabs tested had modulus values lower than 27,579 MPa and in October 2012, approximately 27 percent had modulus values less than 27,579 MPa as presented in Fig. 6b. Based upon these modulus results, it can be concluded that the PCC is distressed [27-28, 31-32].

### Laboratory Analysis of PCC Cores

Fig. 7a to 7c present the average strains in percentage for the length, diameter, and volume caused by submersing the samples in water and sodium hydroxide solutions in accordance with ASTM C1567-13, which was modified as previously mentioned [31]. Increase in length strains as time progressed was measured for samples in both the water and sodium hydroxide solutions as presented in Fig. 7a. Though the mean value for sodium hydroxide solution is higher than the mean value for the water solution, they are not statistically different as presented in Table 5. Increases in diameter strain were measured throughout the 56-day trial period in the sodium hydroxide but were not on certain days during the

**Table 4.** Statistical Results.

| Parameter | Date of Test | Mean (1) | STD. (1) | COV % (2) | Number of Points | Tukey Group (3) | Statistical Result |
|---|---|---|---|---|---|---|---|
| East Bound | | | | | | | |
| AC Overlay | May-07 | 2,917 | 1,123 | 38.5 | 26 | A | Similar |
| | Oct-12 | 2,921 | 975 | 33.4 | 26 | A | |
| PCC | May-07 | 33,652 | 14,567 | 43.3 | 26 | A | Similar |
| | Oct-12 | 37,551 | 9,640 | 25.7 | 26 | A | |
| AC Base Course | May-07 | 6,095 | 2,340 | 38.4 | 26 | A | Different |
| | Oct-12 | 3,768 | 1,212 | 32.2 | 26 | B | |
| Subgrade | May-07 | 183 | 50 | 27.3 | 26 | A | Similar |
| | Oct-12 | 175 | 45 | 25.7 | 26 | A | |
| $SN_{eff}$ | May-07 | 5.5 | 0.3 | 5.6 | 26 | A | Similar |
| | Oct-12 | 5.4 | 0.2 | 3.7 | 26 | A | |
| West Bound | | | | | | | |
| Parameter | Date of Test | Mean (1) | STD. (1) | COV % (2) | Number of Points | Tukey Group (3) | Statistical Result |
| AC overlay | May-07 | 5,295 | 3,469 | 65.5 | 28 | A | Similar |
| | Oct-12 | 4,491 | 1,342 | 29.9 | 28 | A | |
| PCC | May-07 | 44,571 | 11,538 | 25.9 | 28 | A | Similar |
| | Oct-12 | 38,034 | 13,017 | 34.2 | 28 | A | |
| AC Base course | May-07 | 3,222 | 1,467 | 45.5 | 28 | A | Similar |
| | Oct-12 | 2,974 | 1,463 | 49.2 | 28 | A | |
| Subgrade | May-07 | 149 | 47 | 31.5 | 28 | A | Similar |
| | Oct-12 | 160 | 40 | 25 | 28 | A | |
| $SN_{eff}$ | May-07 | 5.7 | 0.2 | 3.5 | 28 | A | Similar |
| | Oct-12 | 5.6 | 0.3 | 5.4 | 28 | A | |

Legend: (1) With the exception of $SN_{eff}$, whose units are dimensionless, the mean and Standard deviation (STD.) are in units of MPa. (2) Coefficient of Variation, (3) In the Tukey groups, similar letters indicate statistical similarities and vice versa.

**Table 5.** Statistical Analysis of Laboratory Samples at 56 Days.

| Parameter Strain | Solution | Mean (%) Strain | STD. (%) Strain | COV (%) (1) | Number of Points | Tukey Group (2) | Statistical Result |
|---|---|---|---|---|---|---|---|
| Length | Water | 0.2527 | 0.1352 | 53.5 | 3 | A | Similar |
| | Sodium Hydroxide | 0.4798 | 0.3820 | 79.6 | 3 | A | |
| Diameter | Water | 0.0323 | 0.0496 | 153.5 | 3 | A | Similar |
| | Sodium Hydroxide | 0.1587 | 0.1334 | 84.1 | 3 | A | |
| Volumetric | Water | 0.2946 | 0.0761 | 25.8 | 3 | B | Different |
| | Sodium Hydroxide | 0.7985 | 0.1954 | 24.5 | 3 | A | |

Legend: (1) Coefficient of variation; (2) In the Tukey groups, similar letters indicate statistical similarities and vice versa.

56-day trial period for the water solution as presented in Fig. 7b. At the 56-day trail period, the statistical analysis revealed that the diameter strains in both solutions were similar as presented in Table 5. Regarding the volumetric strain, the test results indicated that the volumetric strain increased as time progressed for both solutions as presented in Fig. 7c. The statistical analysis revealed that the volumetric strains were statistically different at 56 days with the sodium hydroxide solution having the highest strain (0.8 percent) as presented in Table 5.

The laboratory testing results indicated that the sodium hydroxide solution produced the highest volumetric strain, yet both solutions caused expansions. It is generally accepted that that volumetric strain changes in excess of 0.2 percent will cause detrimental effects in PCC. Therefore, the volumetric strains of 0.8 percent measured in this experiment are large enough to cause detrimental effects in the PCC [1-12, 37].

The PCC pavement is continuing to expand as evidenced by field observations. Laboratory studies of the cores showed that expansion will continue to occur when subjected to elevated temperatures, high alkaline solutions, and sufficiently moist environments.

## Conclusions

The AC overlay proved to be an effective method of mitigating the detrimental effects of ACR and extending the service life of the PCC. Approximately 15 years after the placement of the AC overlay, only minimal transverse cracking, longitudinal cracking, and patching were discovered. On the east bound lanes, the IRI did not change over 15.3 years and its average value was 95 cm/km. The west bound lanes had a different trend indicating an increase in IRI as it aged. Even so, the predicted IRI at 19 years of service would be 126 cm/km indicating a smooth ride according to FHWA standards [30]. The authors postulate that the excellent performance of the

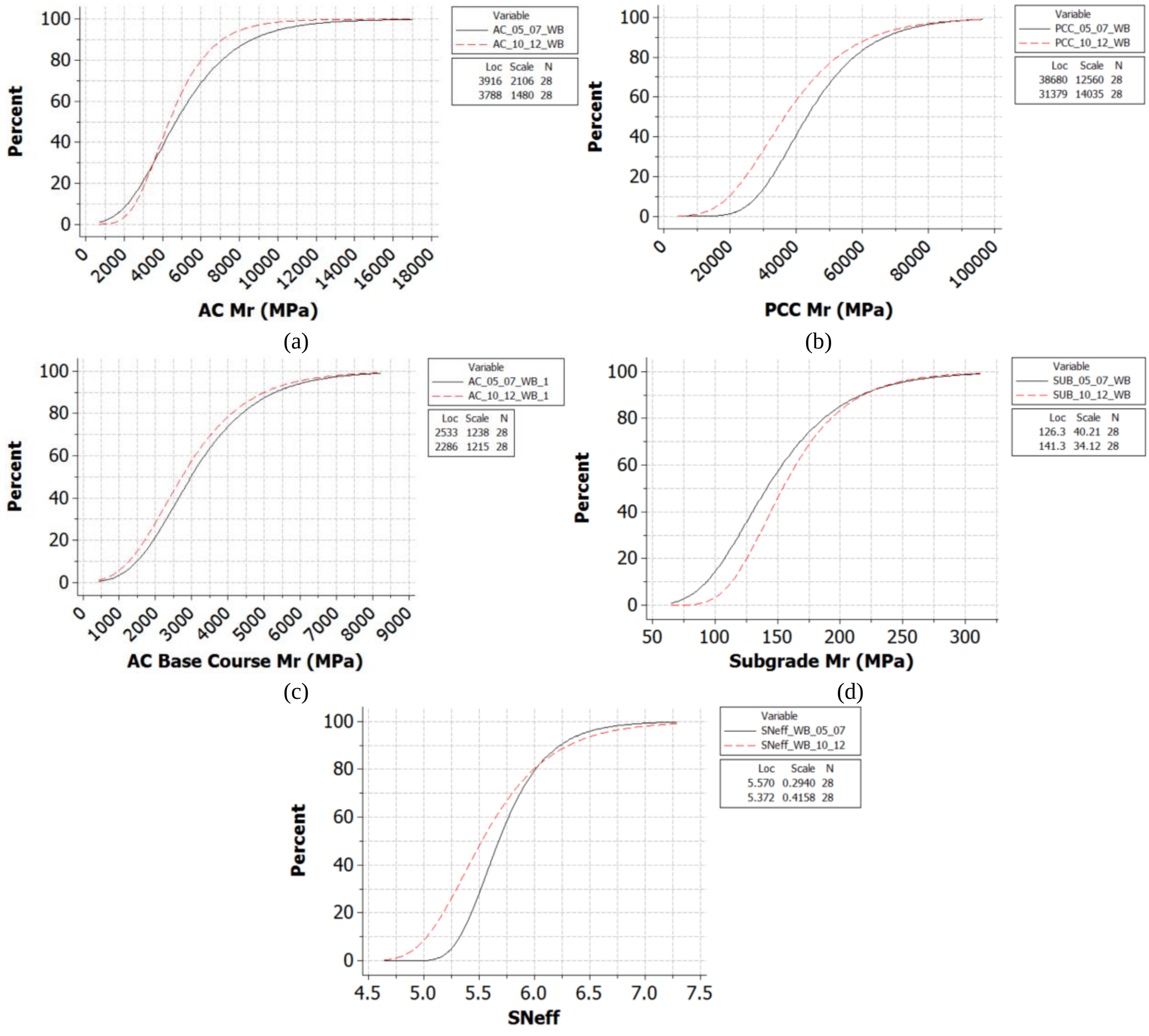


**Fig. 6.** West Bound Histograms: (a) $M_r$ of AC Pavement, (b) $M_r$ of PCC Pavement, (c) $M_r$ of AC Base Course, (d) $M_r$ of Subgrade, (e) $SN_{eff}$ of Pavement Layers.

composite pavement was due factors such as overlaying the PCC early within service life (7.5 years), and sawing and sealing the AC over the PCC joints. The AC overlay also shielded the PCC from surface water and thermally insulated the PCC, thus reducing the detrimental effects of ACR and extending its service life.

With the exception of the AC base course on the east bound roadway, the structural parameters for the AC, PCC, AC base course, subgrade, and $SN_{eff}$ were statistically similar between May 2007 and October 2012. This implies that no deterioration occurred in that 5-year period. Since structural testing was not conducted prior to May 2007, the authors are unable to comment on the amount of deterioration that has occurred since the PCC was constructed. The modulus values did indicate that the PCC was distressed.

Laboratory studies of the cores showed that expansion will continue to occur when subjected to elevated temperatures, high alkaline solutions, and sufficiently moist environments. The laboratory analysis of the PCC cores indicated that significant volumetric strains up to (0.8 percent) occurred when the specimens were tested in water and sodium hydroxide solutions in accordance with a modified version of ASTM C1567-13. Volumetric strains of that magnitude will cause detrimental effects on the PCC, eventually leading to its destruction.

## Acknowledgements

The authors wish to thank LADOTD and LTRC for providing the resources necessary for the project. The assistance of the LTRC pavement research staff members, Mitch Terrell, Shawn Elisar, Glen Gore, and Parker Sanderson along with the Concrete Research Lab staff members Greg Tullier, Norris Rosser, and Craig Johnson is noteworthy.

## References

1. Swenson, E.G. (1957). A Reactive Aggregate Undetected by ASTM Tests, *Proceedings of the Amercian Society for Testing and Materials*, 57, pp. 48-51.

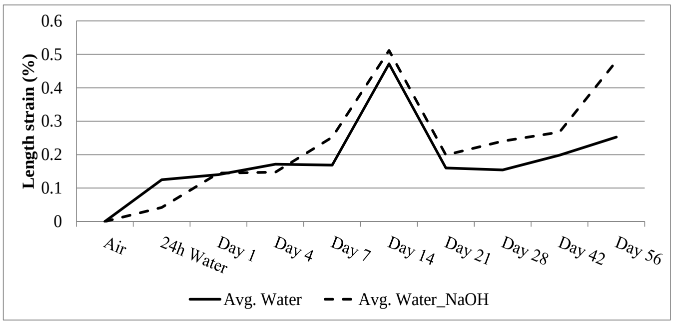


(a)

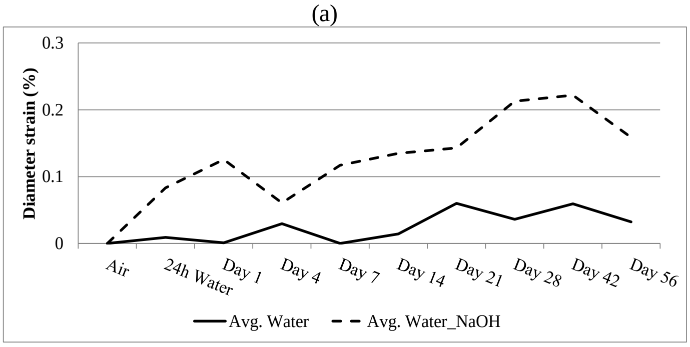


(b)

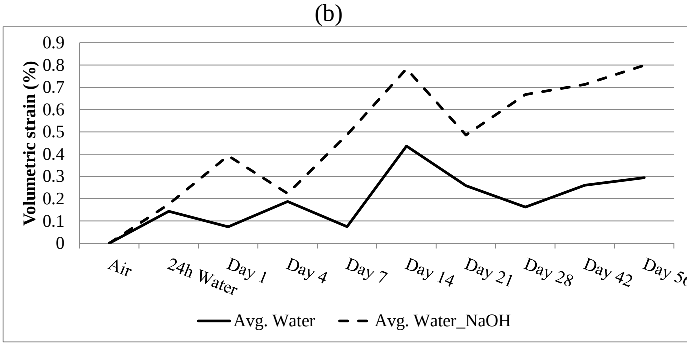


(c)

**Fig. 7.** Laboratory Test Results: (a) Average Length Strain (%), (b) Average Diameter Strain (%), (c) Average Volumetric Strain (%).


2. Swenson, E.G. and Gillott, J.E. (1964). Alkali-Carbonate Rock Reaction, *Highway Research Record*, 45, pp. 21-40.
3. Hadley, D.W. (1961). Alkali Reactivity of Carbonate Rocks: Expansion and Dedolomitization, *Proceedings of the Highway Research Board*, 40, pp. 462-474.
4. Federal Highway Administration (FHWA) (2011). Alkali-Aggregate Reactivity (AAR) Workshops for Engineers and Practitioners, FHWA, U.S. Department of Transportation, Washington, DC, USA, pp. 2-13.
5. Fournier, B. and Berube, M.A. (2000). Alkali-Aggregate Reaction in Concrete: A Review of Basic Concepts and Engineering Implications, *Canadian Journal of Civil Engineering*, 27(2), pp. 167-191.
6. Tang, M., Liu, Z., and Han, S. (1987). Mechanism of Alkali-Carbonate Reaction, *Proceedings of the 7th International Conference on Concrete Alkali-Aggregate Reactions*, Noyes Publications, New Jersey, USA, pp. 275-279.
7. Fournier, B., Berube, M.A., Folliard, K., and Thomas, M. (2010). Report on the Diagnosis, Prognosis, and Mitigation of Alkali-Silica Reaction (ASR) in Transportation Structures, *FHWA-HIF-09-004*, Federal Highway Administration, U.S. Department of Transportation, Washington, DC, USA.
8. Newlon, H. and Sherwood, W. (1964). Methods for Reducing Expansion of Concrete Caused by Alkali-Carbonate Rock Reactions, Symposium on Alkali-Carbonate Rock Reactions, *Highway Research Board*, 45, pp. 134-150.
9. Stanton, T. (1940). Expansion of Concrete through Reaction between Cement and Aggregate, *Proceedings of the American Society of Civil Engineers*, 66(10), pp. 1781-1811.
10. Stark, D. (1994). Alkali-Silica Reaction in Concrete, Tests and Properties of Concrete, *ASTM STP 169C*, pp. 401-409.
11. Haung, M., and Pietruszczak, S. (1999). Modeling of the Thermomechanical Effects of Alkali-Silica Reaction, *Journal of Engineering Mechanics*, 125(4), pp. 476-485.
12. Katayama, T. (2010). The So-called Alkali-Carbonate Reaction (ACR) - Its Mineralogical and Geochemical Details, with Specific Reference to ASR, *Cement and Concrete Research*, 40(4), pp. 643-675.
13. Stark, D., Morgan, B., Okamoto, P., and Diamond, S. (1993). Eliminating or Minimizing Alkali-Silica Reactivity, *SHRP-C-343*, National Research Council, Washington, DC, USA.
14. Folliard, K., Thomas, M, Fournier, B., Kurtis, K., and Ideker, J. (2006). Interim Recommendations for the use of Lithium to Mitigate or Prevent Alkali-Silica Reaction (ASR), *FHWA-HRT-06-073*, Federal Highway Administration, U.S. Department of Transportation, Washington, DC, USA.
15. Berube, M., Chouinard, D., Pigeon, M., Frenette, J., Rivest, M., and Vezina, D. (2002). Effectiveness of Sealers in Counteracting Alkali-Silica Reaction in Highway Median Barriers Exposed to Wetting and Drying, Freezing and Thawing, and Deicing Salts, *Canadian Journal of Civil Engineering*, 29(2), pp. 329-337.
16. Grabe, P., and Oberholster, R. (2000). Programme for the Treatment and Replacement of ASR Affected Concrete Sleepers in the Sishen-Saldanha Railway Line, *Proceedings of the 11th International Conference on Alkali-Aggregate Reaction in Concrete*, Quebec City, Canada, pp. 1059-1068.
17. Rubblization of Portland Cement Concrete Pavements (2006), *Transportation Research Circular*, E-C087, Transportation Research Board, Washington, DC, USA.
18. Sebesta, S., Scullion, T, and Von Holdt, C. (2007). Rubblization for Rehabilitation of Concrete Pavement in Texas: Preliminary Guideline and Case Studies, *FHWA/TX-06/0-4687-1*, Texas Transportation Institute, College Station, Texas, USA.
19. Buncher, M. (2010). Guidelines for Airfield Rubblization, *2010 FAA Worldwide Airport Technology Transfer Conference*, Atlantic City, New Jersey, USA, Asphalt Institute, Lexington, KY, USA.
20. LaForce, R.F. (2006). Performance of Colorado's First Rubblization Project on 1-76 near Sterling, Colorado Department of Transportation, *CDOT-DTD-R-2005-20*, Yeh and Associates, Denver, Colorado, USA.
21. Ceylan, H., Mathews, R., Kota, T., Gopalakrishnan, K., and Coree, B. (2005). Rehabilitation of Concrete Pavements Utilizing Rubblization and Crack and Seat Methods, Center

for Transportation Research and Education, IHRB Project Final Report TR-473, Ames, Iowa, USA.
22. Thompson, M. (1999). Hot Mix Asphalt Overlay Design Concepts for Rubblized Portland Cement Concrete Pavements, *Transportation Research Record*, No. 1684, pp. 147-155.
23. Sheehy, E. (2012). NJ's Innovative Approach for Route I-295 Reconstruction, Presentation at New Jersey Asphalt Paving Conference, Columbus, Ohio, USA.
24. Taylor, J. (2009). Accelerated Concrete Pavement Rubblization and HMA Overlay, Presentation at 85th NESMEA Conference, South Portland, Maine, USA.
25. Khananovich, L., Balbo, J., Johanneck, L., Lederle, R., Marasteanu, M., Saxena, P., Tompkins, D., Vancura, M., Watson, M., Harvey, J., Santero, N., and Signore, J. (2013). Design and Construction Guidelines for Thermally Insulated Concrete Pavements, Center for Transportation Studies, Final Report, University of Minnesota, MN, USA.
26. Johanneck, L., Tompkins, D., Clyne, T. and Khazanovich, L. (2011). Minnesota Road Research Data for Evaluation and Local Calibration of the Mechanistic-Empirical Pavement Design Guide's Enhanced Integrated Climatic Model, *Transportation Research Record*, No. 2226, pp. 30-40.
27. Elseifi, M., and Bandaru, R. (2011). Cost Effective Prevention of Reflective Cracking of Composite Pavements, *FHWA/LA.11/478*, Louisiana Transportation Research Center, Baton Rouge, Louisiana, USA.
28. Khattak, M., Baladi, G., and Sun, X. (2008). Development of Index Based Pavement Performance Models for Pavement Management System (PMS) of LaDOTD, *FHWA/LA.08/460*, Louisiana Transportation Research Center, Baton Rouge, Louisiana, USA.
29. SHRP (1993). Distress Identification Manual for the Long-Term Pavement Performance Project, Strategic Highway Research Program, National Research Council, *SHRP_P_338*, Transportation Research Board, Washington, DC, USA.
30. Federal Highway Administration (FHWA) (1993). Highway Performance Monitoring System, Appendix J, FHWA, U.S. Department of Transportation, Washington, DC, USA.
31. AASHTO (1993). Guide for Design of Pavement Structures, AASHTO, Washington, DC, USA.
32. Yoder, E. (1959). *Principles of Pavement Design*, John Wiley and Sons.
33. Neter, J., Kutner, M., Nachtsheim, C., and Wasserman, W. (1990). *Applied Linear Statistical Models*, 4th Edition, Irwin Publications, New York, New York, USA.
34. Crovetti, J. (2002). Deflection Based Techniques for Jointed Concrete Pavement Systems, *Transportation Research Record*, No. 1809, pp. 3-11.
35. Mohammad, L., Gaspard, K., Hearth, A., and Nazzal, M. (2007). Comparative Evaluation of Subgrade Resilient Modulus for Non-Destructive, In-Situ, and Laboratory Methods, Louisiana Transportation Research Center, Report Number 417, Baton Rouge, Louisiana, USA.
36. Gaspard, K., Icenogle, P., Abadie, C., Zhang, Z., and Elseifi, M. (2013). Historical Performance of Rubblized Jointed Concrete Pavement Overlaid with Asphaltic Concrete in the State Of Louisiana, USA, *International Journal of Pavement Research and Technology*, 6(3), pp. 165-174.
37. ASTM Standard Test Method, C1567-13 (2014). Standard Test Method for Determining the Potential Alkali-Silica Reactivity of Combinations of Cementitious Materials and Aggregate (Accelerated Mortar-Bar Method), ASTM International, West Conshohocken, PA, USA.